

A Time-Varying Iterative Learning Control Scheme

Marina Tharayil and Andrew Alleyne, *Senior Member, IEEE*

Abstract - This paper presents an Iterative Learning Control scheme that uses a time-varying Q-filter. The purpose of the time-varying Q-filter is to utilize the enhanced robustness given by a low bandwidth filter, while taking advantage of the superior performance properties of a high bandwidth Q-filter where needed. Simulations are provided to demonstrate the benefits of the proposed scheme. In addition, stability and convergence issues involved with using a time-varying filter are investigated. Finally the ILC algorithm developed here is implemented on a Microscale Robotic Deposition (μ RD) system to provide experimental verification.

Keywords: Iterative Learning Control, Time varying control, Stability, Robustness, Convergence

I. INTRODUCTION

MANY of the applications of Precision Motion Control (PMC) are repetitive or periodic in nature. For example, robotic applications such as pick and place assembly operations involve repeated iterations of motion trajectories [4], [6], [8]. In these scenarios, it is common to have disturbances that repeat each time the command is given. Conventional feedback controllers, which are more suitable for set-point regulation, would result in repeated errors in these applications. Because of the increased significance of transient performance, feedforward control strategies are usually applied. It is natural then to seek to learn from the previous iterations somehow to improve the performance of the current iteration. Iterative Learning Control (ILC) is one such feedforward algorithm that utilizes previous control and error signals to modify the control input of the current iteration, nominally aiming to converge to zero tracking error. For instance, an Iterative Learning Controller showed 97% improvement over feedback controllers in the Microscale Robotic Deposition system described in Section 4 [3].

Figure 1 shows a schematic of an ILC scheme. Here the subscript j represents the trial or repetition number, and the reference signal $y_d(t)$ is defined on the interval $[0, T]$. At any given repetition, j , a control input of $u_j(t)$ is applied to the system to produce output $y_j(t)$, $t \in [0, T]$, where T is the length of the periodic reference. The input and output of the j^{th} trial are stored in memory and used along with the fixed reference to calculate the input for the $j+1^{\text{th}}$ trial.

Thus the goal of the algorithm is to design an update law to produce the lowest possible error as j tends to infinity. In most ILC systems, it is assumed that the plant initial conditions are reset at the start of every period ($x_j(0) = x_0$). Also, the system is assumed to be stable, or stabilized, using feedback control.

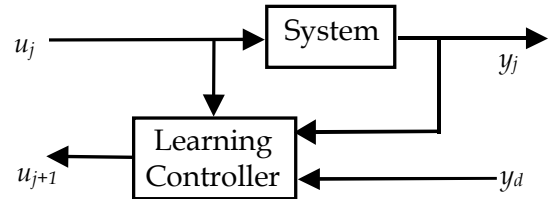


Fig. 1. Learning Control Configuration

As the scale of the operations grow smaller and tolerances tighter, nonlinearities arising due to friction components (coulomb, viscous, and stiction) or force ripples resulting from imperfections in the underlying components take on a more significant role [1], [8], [9]. What's more, often times the controllers are designed based on local linearized models of inherently nonlinear systems. Under these conditions robustness of the controller is highly desirable, in addition to its ability to render the required performance. Thus it is clear that development of ILC algorithms that provide additional robustness and good performance will be directly advantageous to many of these emerging technologies. The time-varying ILC scheme presented in this paper is one such algorithm that can extend the robustness and performance boundaries given by traditional linear time-invariant (LTI) ILC algorithms. The general ILC problem formulation and the structure of the time-varying ILC scheme are presented next.

A general first order ILC update law is of the form:

$$u_{j+1}(t) = f_L(u_j, e_j) \quad (1)$$

where

$$e_j(t) = y_d(t) - y_j(t) \quad (2)$$

Three attributes that are considered are:

- 1) *Stability / Convergence*: Existence of $u^*(t)$ such that

$$\lim_{j \rightarrow \infty} u_j(t) = u^*(t) \quad (3)$$

- 2) *Performance*: Existence of $\varepsilon \geq 0$ such that the converged error $e^*(t)$ satisfies

$$\|e^*(t)\|_p < \varepsilon \quad (4)$$

This work is supported in part by NSF grant DMI-0328162

The authors are with the department of Mechanical and Industrial Engineering at the University of Illinois at Urbana Champaign, Urbana IL, 61801. (Corresponding author e-mail: alleyne@uiuc.edu)

3) *Robustness*: Satisfaction of stability / convergence condition in the presence of plant (P) uncertainties:

$$\tilde{P} = P(1 + \Delta) \quad (5)$$

The general traditional formulation for a linear ILC update law can be written in the following form [5].

$$u_{j+1}(t) = Q[u_j(t) + L_e e_j(t)] \quad (6)$$

Here learning parameters Q and L_e are LTI operators. It has been shown that such formulation results in a trade off between robustness and performance [4]. For example, using Laplace transforms to represent the signals u , e and the LTI Transfer Functions $Q(s)$, $L_e(s)$, it can be shown that increasing the bandwidth of $Q(s)$ results in improved performance at the cost of robustness, and vice versa.

This paper proposes to circumvent the frequency domain bandwidth conditions by using a time-varying Q-filter. The ILC update law proposed uses one form of a time-varying Q-filter:

$$u_{j+1}(t) = Q(t)[u_j(t) + L_e e_j(t)] \quad (7)$$

The scheme presented here modifies the traditional formulation to give the designer an additional degree of freedom by allowing him or her to vary the balance between performance and robustness at each point in the period. This can be very beneficial systems with either (1) localized nonlinear behavior entering at specific regions within the period or, (2) system model accuracy varying during the period – i.e. $\Delta = \Delta(t)$. Another scenario where the time-varying Q-filter is advantageous is when the reference signal, $y_d(t)$, has significant changes in its frequency content during the course of the period. For example, in such case the bandwidth of the Q-filter can be increased when $y_d(t)$ has high frequencies for enhanced performance. In the case where there are high uncertainties at known portions within the period, the bandwidth of the Q-filter should be decreased for additional robustness.

The remainder of the paper is organized as follows. Section 2 introduces the ILC scheme and develops the stability/convergence conditions for discrete-time systems. Next, the design procedure for such a scheme is demonstrated using a motivational example in Section 3, after which experimental results on the μ RD section are reported in Section 4. Section 5 concludes the paper.

II. ILC ANALYSIS

A discrete formulation of the system is used in this investigation as it is more natural for digital implementation. Consider a stable linear, time-invariant, causal discrete-time plant P of the form:

$$Y(z) = P(z)U(z) \quad (8)$$

where z^{-1} is the standard delay operator. $P(z)$ has state space representation (9), and its input output behavior can

be written in the form of a convolution sum shown in (10). Here k is the discrete time index and n is the number of time steps in a period.

$$\begin{aligned} x(k+1) &= Ax(k) + Bu(k) & k &= 0, 1, \dots, n-1 \\ y(k) &= Cx(k) & k &= 1, \dots, n \end{aligned} \quad (9)$$

$$y(k) = CA^k x(0) + \sum_{i=1}^{k-1} CA^{k-i-1} Bu(i) \quad k = 0, 1, \dots, n \quad (10)$$

Assuming zero initial conditions, $P(z)$ can be written as follows [6], [7]. Here p_i , sometimes called the Markov parameters of the plant, are given by $CA^{i-1}B$.

$$P(z) = p_1 z^{-1} + p_2 z^{-2} + p_3 z^{-3} + \dots \quad (11)$$

Note that it is assumed the plant is of relative degree 1 here. For a transfer function of relative degree r , the first nonzero element will be multiplied by z^{-r} . Again, letting n be the number of time steps in the period T , and j be the iteration number, define vectors \hat{y}_j , \hat{y}_d and \hat{u}_j as follows:

$$\hat{y}_j = \begin{bmatrix} y_j(1) \\ y_j(2) \\ \vdots \\ y_j(n) \end{bmatrix}; \hat{y}_d = \begin{bmatrix} y_d(1) \\ y_d(2) \\ \vdots \\ y_d(n) \end{bmatrix}; \hat{u}_j = \begin{bmatrix} u_j(0) \\ u_j(1) \\ \vdots \\ u_j(n-1) \end{bmatrix} \quad (12)$$

Then the linear plant (8) can be written as follows:

$$\hat{y}_j = P\hat{u}_j + \hat{d} \quad (13)$$

where \hat{d} is a vector of the form (12) containing the effects of periodic disturbance, and P is a matrix of Markov parameters of the plant.

$$P = \begin{bmatrix} p_1 & 0 & \dots & 0 \\ p_2 & p_1 & \dots & 0 \\ \vdots & \vdots & \ddots & \vdots \\ p_n & p_{n-1} & \dots & p_1 \end{bmatrix} \quad (14)$$

The most general ILC update law can be written in the form:

$$\hat{u}_{j+1} = Q(\hat{u}_j + L_e \hat{e}_j) \quad (15)$$

where Q and L_e are $n \times n$ matrices that determine the updated control vector of the $j+1^{\text{th}}$ iteration based on the current control and error vectors.

Theorem 1: A necessary and sufficient (N&S) condition for convergence of \hat{u}_j to \hat{u}^* as $j \rightarrow \infty$ is given by:

$$|\lambda_i(Q(I - L_e P))| < 1 \quad \forall i = 1, 2, \dots, n \quad (16)$$

Proof:

A shift operator is defined as follows and applied to \hat{y}_j :

$$\delta_j \hat{f} = \hat{f}_j - \hat{f}_{j-1} \quad (17)$$

$$\delta_j \hat{y} = \hat{y}_j - \hat{y}_{j-1} = [P\hat{u}_j + \hat{d}] - [P\hat{u}_{j-1} + \hat{d}] = P\delta_j \hat{u} \quad (18)$$

The shift operator is applied to the control vector next.

$$\begin{aligned} \delta_{j+1} \hat{u} &= \hat{u}_{j+1} - \hat{u}_j \\ &= Q[\hat{u}_j + L_e \hat{e}_j] - Q[\hat{u}_{j-1} + L_e \hat{e}_{j-1}] \\ &= Q[\delta_j \hat{u} + L_e(\hat{y}_d - \hat{y}_j)] - L_e(\hat{y}_d - \hat{y}_{j-1}) \\ &= Q(\delta_j \hat{u} - L_e \delta_j \hat{y}) = Q(I - L_e P)\delta_j \hat{u} \end{aligned} \quad (19)$$

It is now obvious that $\delta_j \hat{u}$ converges to zero if and only if all eigenvalues of the matrix $Q(I - L_e P)$ lie within the unit circle. ■

The above theorem is a well-known N&S condition for convergence of the ILC law. The matrices Q and L_e in (15) were of the most general form. For an ILC update law described by causal, LTI discrete transfer functions, matrices Q and L_e will be of the form

$$L_e = \begin{bmatrix} l_0 & 0 & \cdots & 0 \\ l_1 & l_0 & \cdots & 0 \\ \vdots & \vdots & \ddots & \vdots \\ l_{n-1} & l_{n-2} & \cdots & l_0 \end{bmatrix}; \quad Q = \begin{bmatrix} q_0 & 0 & \cdots & 0 \\ q_1 & q_0 & \cdots & 0 \\ \vdots & \vdots & \ddots & \vdots \\ q_{n-1} & q_{n-2} & \cdots & q_0 \end{bmatrix} \quad (20)$$

It is assumed the transfer functions $L_e(z)$ and $Q(z)$ are of relative degree zero, or the matrices have been shifted accordingly. In this case, the stability transfer function $Q(I - L_e P)$ is lower triangular, with identical values across its diagonal. This leads to the following theorem.

Theorem 2: The N&S condition for convergence of the ILC system defined by (13) and the update law (20) is

$$|q_0(1 - l_0 p_1)| < 1 \quad (21)$$

Proof:

The eigenvalues of a lower triangular matrix are its diagonal elements. The diagonal elements of $Q(I - L_e P)$ are $q_0(1 - l_0 p_1)$. ■

A: Time-Varying Q-filter:

Define a time-varying Q-filter that switches between two causal LTI filters $Q_a(z)$ and $Q_b(z)$ as shown in (23). Here $q_{a,i}$ and $q_{b,i}$ represent the Markov parameters of filter Q_a and Q_b respectively

Theorem 3: The N&S conditions for convergence of the ILC system defined by (13) using the update law (15) with Q filter of the form (23) is given by:

$$|q_{a,0}(1 - l_0 p_1)| < 1 \text{ and } |q_{b,0}(1 - l_0 p_1)| < 1 \quad (22)$$

Proof:

Same as Theorem 2. ■

$$Q_w = \left. \begin{array}{cccccc} q_{a,0} & 0 & 0 & \cdots & & 0 \\ q_{a,1} & q_{a,0} & 0 & \cdots & & 0 \\ \vdots & \vdots & \ddots & \ddots & & \vdots \\ q_{b,p} & \cdots & q_{b,1} & q_{b,0} & 0 & \\ \vdots & \cdots & \vdots & \vdots & \ddots & \ddots \\ q_{a,n-2} & \cdots & & & q_{a,1} & q_{a,0} & 0 \\ q_{a,n-1} & q_{a,n-2} & \cdots & & \cdots & q_{a,1} & q_{a,0} \end{array} \right\} \begin{array}{l} Q_a \\ Q_b \\ Q_a \end{array} \quad (23)$$

It can be seen that this result can easily be extended to a system switching between m Q-filters. It is noted here that the use of non-causal filters results in full matrices Q and L_e , and (16) gives the N&S condition for convergence in such case.

B: Performance and Robustness

Theorem 4: For the ILC system described by (13) and the general update law (15), the converged \hat{u}^* and \hat{e}^* are given by:

$$\hat{u}^* = \lim_{j \rightarrow \infty} \hat{u}_j = [I - Q + QL_e P]^{-1} QL_e (\hat{y}_d - \hat{d}) \quad (24)$$

$$\hat{e}^* = \lim_{j \rightarrow \infty} \hat{e}_j = [I - P[I - Q + QL_e P]^{-1} QL_e] (\hat{y}_d - \hat{d}) \quad (25)$$

Proof:

Using (15) and (13), for the converged \hat{u}^* and \hat{e}^* , we have:

$$\hat{u}^* = Q(\hat{u}^* + L_e \hat{e}^*); \quad \hat{e}^* = \hat{y}_d - \hat{y}^* \quad (26)$$

$$\hat{u}^* = Q(\hat{u}^* - L_e P \hat{u}^* - L_e \hat{d} + L_e \hat{y}_d) \quad (27)$$

$$\Rightarrow \hat{u}^* = [I - Q + QL_e P]^{-1} QL_e (\hat{y}_d - \hat{d}) \quad (28)$$

$$\begin{aligned} \hat{e}^* &= \hat{y}_d - (P\hat{u}^* + \hat{d}) \\ &= (\hat{y}_d - \hat{d}) - P[I - Q + QL_e P]^{-1} QL_e (\hat{y}_d - \hat{d}) \end{aligned} \quad (29)$$

$$\Rightarrow \hat{e}^* = [I - P[I - Q + QL_e P]^{-1} QL_e] (\hat{y}_d - \hat{d}) \quad (30)$$

A measure of performance is given by the smallest $\varepsilon \geq 0$ such that (4) is satisfied, and a robustness measure can be viewed as the largest Δ such that \tilde{P} defined in (5) satisfies (3). Given variations in y_d and d within the period, the rows of Q can be adjusted to minimize the converged error for a given set of y_d and d . Similarly, if plant uncertainties are high during known parts of the period, changing q_0 for the corresponding rows ensures stability for the perturbed system. Some suggestions on how to design a time-varying Q-filter that takes advantage of this freedom are given in the following section.

III. DESIGN AND IMPLEMENTATION

A schematic of the LTI ILC is shown in Figure 2. The ideal design for a model based ILC design is to let $L_e = P^{-1}$ and $Q = I$. It can be readily checked that this satisfies the stability conditions and results in zero steady state error. However, in real systems, exact inversion of the plant dynamics is almost never realizable, especially using a causal L_e . Thus it is recommended to use a low pass filter, Q , to ensure stability conditions are met even in the face of uncertainties. However, introducing the Q-filter results in loss of zero steady state error, thereby initiating the trade-off between performance and robustness. This trade-off, as well as the benefit of utilizing a time-varying Q-filter are demonstrated using an example in 3.1

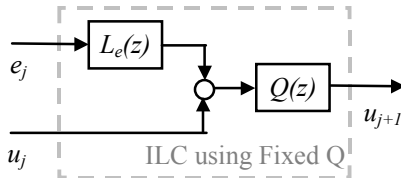


Fig. 2. Causal, LTI ILC structure

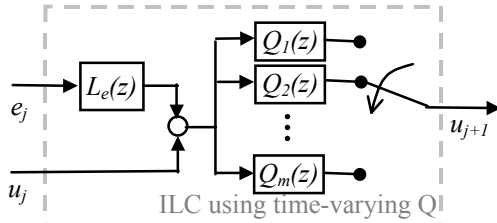


Fig. 3. Causal, LTV ILC structure

The time-varying ILC scheme proposed in this paper can be represented as shown in Figure 3. The time-varying Q-filter, Q_n , effectively switches between fixed filters Q_1, Q_2, \dots, Q_m during the course of each iteration. It is assumed that the switching order is fixed for all iterations. The matrix representation of Q_n will be of the form (23). The filters Q_1, Q_2, \dots, Q_m are chosen as follows. Let Q_i be a low pass filter with cut-off frequency ω_i , where $\omega_1 < \omega_2 < \dots < \omega_m$. The switching order is to be such that Q_1 is the nominal filter (lowest cut-off frequency for highest robustness) and filters of higher bandwidth are used when necessary to meet performance requirements. Thus the switching order of Q_i is based on the desired bandwidth at any given time, as shown in Figure 4. A smooth bandwidth profile is recommended to preserve continuity of signals. The design of the bandwidth profile can be based on the frequency content of y_d and known periodic disturbances, d .

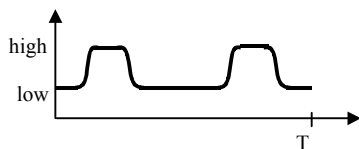


Fig. 4. Example bandwidth profile for Q_n .

A: Simulation Example

The following example problem is based on the linearized dynamic model for a linear motor used by the μ RD system described in [2],[3]. Given a true plant \tilde{P} , and a simplified model $P(z)$, the goal is to design an ILC algorithm for output tracking. The simplified model (31), designed for sample time of 0.001sec, does not include the high frequency structural resonances and is assumed to be stable. The true plant transfer function is given by (32) and the desired trajectory, y_d , is shown in Figure 5. Note that robustness of the ILC update law is critical here because the design is based on a simplified linear model, as is common in practice. ILC update laws using two different fixed Q-filters, and a time-varying one that varies between the two values, are offered to demonstrate some of the advantages of using a time-varying Q-filter. These update laws are simulated on the simplified plant model and the true model for comparison.

$$P(z) = \frac{10^{-4} [8.64z^3 - 6.24z^2 - 8.46z + 6.40]}{z^4 - 3.66z^3 + 5.06z^2 - 3.14z + 0.74} \quad (31)$$

$$= 0.0009z^{-1} + 0.0025z^{-2} + 0.0041z^{-3} + \dots$$

$$\tilde{P}(z) = 0.0008z^{-1} + 0.0022z^{-2} + 0.0030z^{-3} + \dots$$

$$= \frac{10^{-3} [0.82z^7 - 3.8z^6 + 6.3z^5 - 3.2z^4 - 3.3z^3 + 5.5z^2 - 2.9z + 0.56]}{z^8 - 7.28z^7 + 23.4z^6 - 43.44z^5 + 50.96z^4 - 38.71z^3 + 18.6z^2 - 5.17z + 0.63} \quad (32)$$

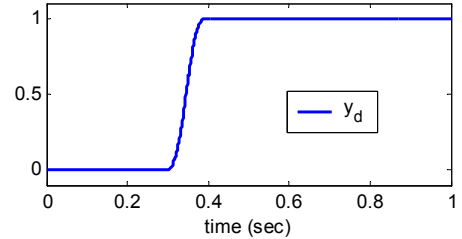


Fig. 5. Desired Trajectory, y_d

We let $L_e \approx P^{-1}$ as follows to preserve causality:

$$L_e(z) = \frac{P^{-1}(z)}{(z/0.85 + 1)} = 10^4 \times [0.0984 - 0.3724z^{-1} + \dots] \quad (33)$$

It is noted that the stability condition (21) can be met using the above L_e without the use of a Q-filter. However, this can still result in bad learning transients where the error can grow to be very large before converging [10]. A low pass Q-filter tends to improve the transient performance at the cost of increased conservatism. Furthermore, a low-pass Q-filter is important in actual systems for additional robustness as well as noise attenuation. Two first order butterworth filters of cut-off frequencies 100 rads/sec and 2000 rads/sec each are chosen as follows:

$$Q_{low}(z) = \frac{0.048(z+1)}{z-0.9047} = 0.05 + 0.09z^{-1} + \dots \quad (34)$$

$$Q_{high}(z) = \frac{0.609(z+1)}{z+0.218} = 0.61 + 0.48z^{-1} + \dots \quad (35)$$

As was mentioned above, the N&S condition (21) can be met using either filter. The RMS values of converged errors for either case can be calculated using (25).

$$q_{low,0}(1 - l_0 p_1) = 0.0071; \hat{e}_{low,RMS}^* = 0.0716 \quad (36)$$

$$q_{high,1}(1 - l_1 p_1) = 0.0913; \hat{e}_{high,RMS}^* = 0.0028 \quad (37)$$

Figure 6 shows the RMS value of the error of the nominal system as a function of iteration number for both the above cases, as well as error evolution using a time-varying Q-filter. The time-varying Q-filter, Q_{tv} , of the form (23), is composed of a set of first order butterworth filters with bandwidth ranging from that of Q_{low} to that of Q_{high} , as shown in Figure 9. It is verified that condition (22) is satisfied by the set of filters in Q_{tv} . Details on the design of Q_{tv} are given shortly. It can be seen that the performance using the time-varying Q-filter is comparable to that of the ILC update law using fixed high bandwidth Q-filter on the ideal linear plant.

$$\hat{e}_{iv,RMS}^* = 0.0031 \quad (38)$$

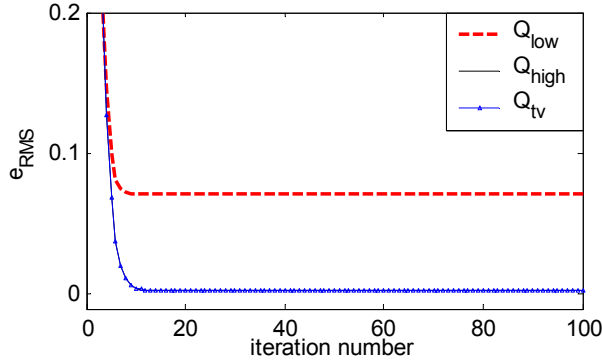


Fig. 6. RMS values of $e(t)$ per iteration using P

Next, the same ILC laws are applied to the actual plant, \tilde{P} , and the evolution of the error is plotted in Figure 7. Clearly, the ILC law with time-varying Q-filter performed better than either fixed filter here. The ILC update law using the fixed high bandwidth filter exhibits very poor learning transients. The RMS value of the error reaches a peak value of approximately 2500 by the 200th iteration before convergence. Some insight can be gained from the converged error plots shown in Figure 8. The fixed law with Q_{low} shows good learning transients but results in large errors between $t=0.3$ sec and $t=0.45$ sec, coinciding with the high frequency content in y_d . The fixed law with Q_{high} , which would have had better tracking performance, results in poor learning transients. The time varying update law results in tracking comparable to the fixed law using Q_{high} , along with learning transients similar to the fixed law using Q_{low} . This clearly demonstrates that the time varying Q-

filter can simultaneously provide better robustness and performance than either LTI Q-filter.

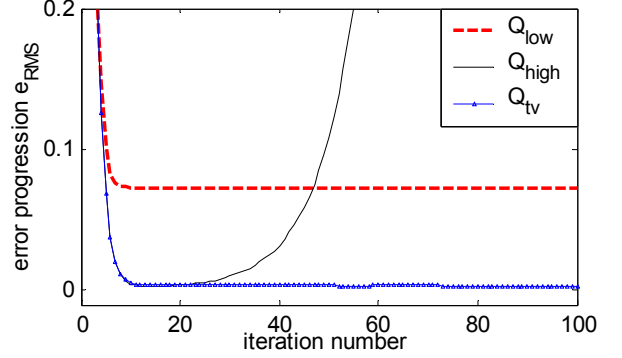


Fig. 7. RMS values of $e(t)$ per iteration using \tilde{P}

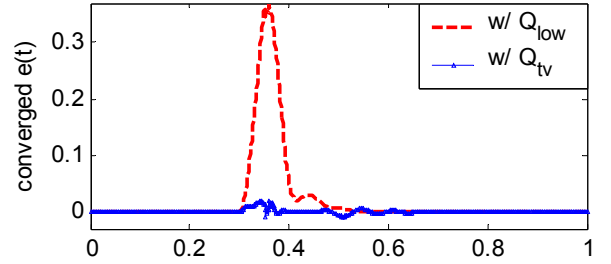


Fig. 8. Converged value of $e(t)$ using \tilde{P}

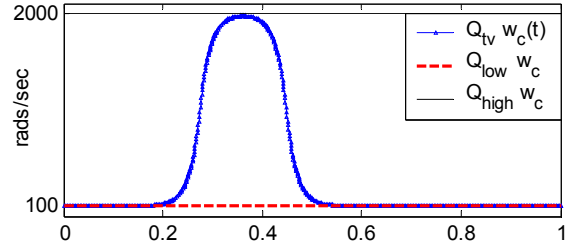


Fig. 9. Bandwidth profile of time-varying Q-filter.

A time frequency distribution of y_d reveals high frequency content during the interval $t \in (0.3, 0.45)$. It is obvious that high frequency control is necessary during this interval for accurate tracking of y_d . Therefore, the time-varying Q-filter used in the above example consists of a set of low-pass filters with varying bandwidth as shown in Figure 9. Once again, the idea is that the bandwidth is increased when needed to improve performance while nominally remaining at the low value for increased robustness.

IV. EXPERIMENTAL RESULTS

The Microscale Robotic Deposition (μ RD) system uses robotic positioning to deposit an ‘ink’ for 3-D construction of complex parts of small dimensions [2],[3]. A schematic of the system is shown in Figure 10. Very precise X-Y-Z axis positioning of the robot end effector is required for the accurate manufacturing of the desired parts. The algorithm described in this paper is applied to control the X-axis

position here. The simplified model used for the X-axis positioning system dynamics is shown in (39). The actual system, in addition to having high frequency resonances, experiences friction and other nonlinear effects.

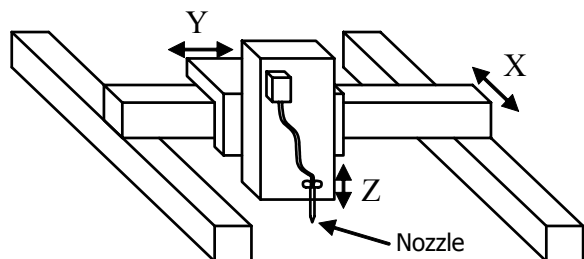


Fig. 10. Schematic of μ RD system

$$P_x(z) = 8.8 \times 10^{-4} \frac{z^5 - 2.90z^4 + 1.98z^3 + 1.67z^2 - 2.68z + 0.93}{z^6 - 5.72z^5 + 13.73z^4 - 17.74z^3 + 13.02z^2 - 5.15z + 0.86} \quad (39)$$

The ILC update algorithm uses a PD learning law as described in [2] with $K_{pX} = 1.779$ and $K_{dX} = 111$. The reference trajectory shown in Figure 5 is used for a 1mm change in y . The time-varying Q-filter used is of the form shown in Figure 9 with the cut-off frequency of Q_{low} at 50 rads/sec, and that of Q_{high} at 300 rads/sec. Figures 11 and 12 demonstrate the improved performance obtained by increasing the bandwidth for a short period, $t \in [-0.3, 0.45]$.

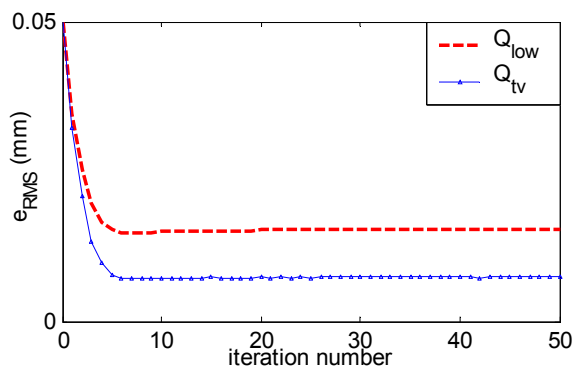


Fig. 11. Experimentally obtained RMS values of $e(t)$

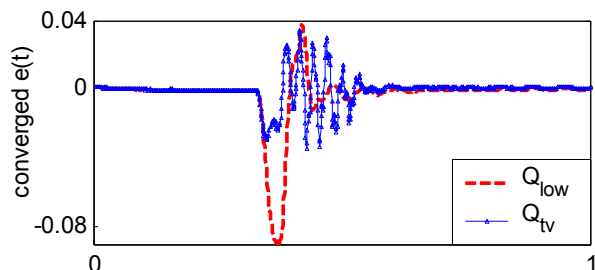


Fig. 12. Converged values of $e(t)$

V. CONCLUSIONS

This paper presents a new tool for PMC applications by developing the time-varying Q-filter. Convergence conditions as well as performance and robustness criteria were formulated for the proposed ILC scheme. The design

issues involved were highlighted using an instructional example based on a Microscale Robotic Deposition system at the University of Illinois. Finally, actual data from implementing an ILC with time-varying Q-filter is shown to verify the effectiveness of the proposed scheme.

ACKNOWLEDGMENT

The authors would like to express their gratitude to Douglas Bristow for help with obtaining the experimental data, and both Douglas Bristow and Danian Zheng for useful discussions related to this work. The time-varying Q-filter concept was originally empirically implemented in an Adaptive ILC scheme developed in [11].

REFERENCES

- [1] Bleuler, H., R. Clavel, J.-M. Breguet, H. Langen, E. Pernette, "Issues in Precision Motion Control and Microhandling, *Proceedings of the 2000 IEEE International Conference on Robotics & Automation*, pp. 959-964, April 2000.
- [2] Bristow, D., A. Alleyne, and D. Zheng, "Control of a Microscale Deposition Robot Using a New Adaptive Time-Frequency Filtered Iterative Learning Control", *Proceedings of the American Control Conference*, July 2004.
- [3] Bristow, D., "Modeling and Control of a Microscale Robotic Deposition Manufacturing System", Masters Thesis, University of Illinois at Urbana-Champaign, 2003.
- [4] Elci, H., R. Longman, M. Phan, J.-N. Juang, and R. Ugoletti, "Simple Learning Control Made Practical by Zero-Phase Filtering: Applications to Robotics", *IEEE Transactions on Circuits and Systems*, Vol. 49, No. 6, pp. 753-767, June 2002.
- [5] Moore, K. L., *Iterative Learning Control for Deterministic Systems*, London: Springer-Verlag, 1993.
- [6] Moore, K. L., "Iterative Learning Control: An Expository Overview," *Applied and Computational Controls, Signal Processing, and Circuits*, Vol. 1, No. 1, pp. 425-488, 1998.
- [7] Phan, M. Q., R. W. Longman, and K. L. Moore, "Unified Formulation of Linear Iterative Learning Control," *Advances in Astronautical Sciences*, Vol. 106, pp. 93-111, 2000.
- [8] Tan, K. K., H. Kou, Y. Chen, and T. H. Lee, "High Precision Linear Motor Control via Relay Tuning and Iterative Learning Based on Zero-Phase Filtering", *IEEE Transactions on Control Systems Technology*, Vol. 9, No. 2, March 2001.
- [9] Tomizuka, M., "On the Compensation of Friction Forces in Precision Motion Control", *Proceedings of the Asia-Pacific Workshop on Advances in Motion Control*, pp. 69-74, 1993
- [10] Huang, Y-C and R. Longman, "The Source of the Often Observed Property of Initial Convergence Followed by Divergence in Learning and Repetitive Control", *Advance in Astronautical Sciences*, Vol. 90, No. 1, pp. 555-572, 1996.
- [11] Zheng, D., "Iterative Learning Control of an Electro-Hydraulic Injection Molding Machine with Smooth Fill-to-Pack Transition and Adaptive Filtering", PhD Thesis, University of Illinois at Urbana-Champaign, 2002.